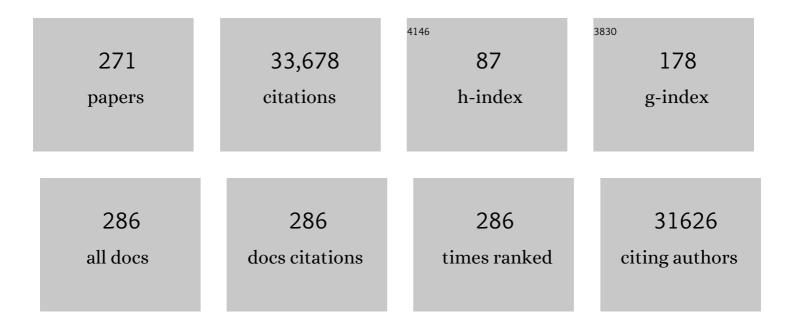
Jianfang F Wang

List of Publications by Year in descending order

Source: https://exaly.com/author-pdf/3577203/publications.pdf Version: 2024-02-01



#	Article	IF	CITATIONS
1	Indium phosphide nanowires as building blocks for nanoscale electronic and optoelectronic devices. Nature, 2001, 409, 66-69.	27.8	3,256
2	Growth of nanowire superlattice structures for nanoscale photonics and electronics. Nature, 2002, 415, 617-620.	27.8	2,562
3	Gold nanorods and their plasmonic properties. Chemical Society Reviews, 2013, 42, 2679-2724.	38.1	1,576
4	Shape- and Size-Dependent Refractive Index Sensitivity of Gold Nanoparticles. Langmuir, 2008, 24, 5233-5237.	3.5	1,126
5	Diameter-controlled synthesis of single-crystal silicon nanowires. Applied Physics Letters, 2001, 78, 2214-2216.	3.3	1,078
6	Metal/Semiconductor Hybrid Nanostructures for Plasmonâ€Enhanced Applications. Advanced Materials, 2014, 26, 5274-5309.	21.0	926
7	New Reaction Pathway Induced by Plasmon for Selective Benzyl Alcohol Oxidation on BiOCl Possessing Oxygen Vacancies. Journal of the American Chemical Society, 2017, 139, 3513-3521.	13.7	693
8	Composite mesostructures by nano-confinement. Nature Materials, 2004, 3, 816-822.	27.5	626
9	Plasmonic gold mushroom arrays with refractive index sensing figures of merit approaching the theoretical limit. Nature Communications, 2013, 4, 2381.	12.8	612
10	Plasmonic Harvesting of Light Energy for Suzuki Coupling Reactions. Journal of the American Chemical Society, 2013, 135, 5588-5601.	13.7	597
11	Efficient Ammonia Electrosynthesis from Nitrate on Strained Ruthenium Nanoclusters. Journal of the American Chemical Society, 2020, 142, 7036-7046.	13.7	542
12	Tailoring Longitudinal Surface Plasmon Wavelengths, Scattering and Absorption Cross Sections of Gold Nanorods. ACS Nano, 2008, 2, 677-686.	14.6	527
13	Understanding the Photothermal Conversion Efficiency of Gold Nanocrystals. Small, 2010, 6, 2272-2280.	10.0	505
14	Active Plasmonics: Principles, Structures, and Applications. Chemical Reviews, 2018, 118, 3054-3099.	47.7	483
15	Strong Polarization Dependence of Plasmon-Enhanced Fluorescence on Single Gold Nanorods. Nano Letters, 2009, 9, 3896-3903.	9.1	388
16	Plasmon-Controlled Fluorescence: Beyond the Intensity Enhancement. Journal of Physical Chemistry Letters, 2012, 3, 191-202.	4.6	388
17	High-Efficiency "Working-in-Tandem―Nitrogen Photofixation Achieved by Assembling Plasmonic Gold Nanocrystals on Ultrathin Titania Nanosheets. Journal of the American Chemical Society, 2018, 140, 8497-8508.	13.7	382
18	Growth of Tetrahexahedral Gold Nanocrystals with High-Index Facets. Journal of the American Chemical Society, 2009, 131, 16350-16351.	13.7	357

#	Article	IF	CITATIONS
19	Selective Shortening of Single-Crystalline Gold Nanorods by Mild Oxidation. Journal of the American Chemical Society, 2006, 128, 5352-5353.	13.7	305
20	Heteroepitaxial Growth of High-Index-Faceted Palladium Nanoshells and Their Catalytic Performance. Journal of the American Chemical Society, 2011, 133, 1106-1111.	13.7	287
21	Synthesis and optical properties of gallium arsenide nanowires. Applied Physics Letters, 2000, 76, 1116-1118.	3.3	279
22	Synthetic Control of the Diameter and Length of Single Crystal Semiconductor Nanowires. Journal of Physical Chemistry B, 2001, 105, 4062-4064.	2.6	265
23	Plasmon-enhanced chemical reactions. Journal of Materials Chemistry A, 2013, 1, 5790.	10.3	257
24	pH ontrolled Reversible Assembly and Disassembly of Gold Nanorods. Small, 2008, 4, 1287-1292.	10.0	256
25	Ordered Gold Nanostructure Assemblies Formed By Droplet Evaporation. Angewandte Chemie - International Edition, 2008, 47, 9685-9690.	13.8	244
26	A General Approach to Mesoporous Metal Oxide Microspheres Loaded with Noble Metal Nanoparticles. Angewandte Chemie - International Edition, 2012, 51, 6406-6410.	13.8	237
27	Gold Nanorods: The Most Versatile Plasmonic Nanoparticles. Chemical Reviews, 2021, 121, 13342-13453.	47.7	237
28	High-Photoluminescence-Yield Gold Nanocubes: For Cell Imaging and Photothermal Therapy. ACS Nano, 2010, 4, 113-120.	14.6	233
29	(Gold Core)@(Ceria Shell) Nanostructures for Plasmon-Enhanced Catalytic Reactions under Visible Light. ACS Nano, 2014, 8, 8152-8162.	14.6	230
30	Unraveling the Evolution and Nature of the Plasmons in (Au Core)–(Ag Shell) Nanorods. Advanced Materials, 2012, 24, OP200-7.	21.0	225
31	Site-Selective Growth of Crystalline Ceria with Oxygen Vacancies on Gold Nanocrystals for Near-Infrared Nitrogen Photofixation. Journal of the American Chemical Society, 2019, 141, 5083-5086.	13.7	222
32	High Internal Phase Emulsions Stabilized Solely by Microgel Particles. Angewandte Chemie - International Edition, 2009, 48, 8490-8493.	13.8	221
33	Size-Dependent Photoluminescence from Single Indium Phosphide Nanowires. Journal of Physical Chemistry B, 2002, 106, 4036-4039.	2.6	215
34	Production of Monodisperse Gold Nanobipyramids with Number Percentages Approaching 100% and Evaluation of Their Plasmonic Properties. Advanced Optical Materials, 2015, 3, 801-812.	7.3	215
35	Porous Singleâ€Crystalline Palladium Nanoparticles with High Catalytic Activities. Angewandte Chemie - International Edition, 2012, 51, 4872-4876.	13.8	206
36	Templated Synthesis of Highly Ordered Mesostructured Nanowires and Nanowire Arrays. Nano Letters, 2004, 4, 2337-2342.	9.1	205

#	Article	IF	CITATIONS
37	Growth of Gold Bipyramids with Improved Yield and Their Curvatureâ€Directed Oxidation. Small, 2007, 3, 2103-2113.	10.0	203
38	<i>In vitro</i> effect of CTAB- and PEG-coated gold nanorods on the induction of eryptosis/erythroptosis in human erythrocytes. Nanotoxicology, 2012, 6, 847-856.	3.0	194
39	Plasmon–molecule interactions. Nano Today, 2010, 5, 494-505.	11.9	193
40	A General Approach to the Synthesis of Gold–Metal Sulfide Core–Shell and Heterostructures. Angewandte Chemie - International Edition, 2009, 48, 2881-2885.	13.8	191
41	Observing Plasmonicâ ´`Molecular Resonance Coupling on Single Gold Nanorods. Nano Letters, 2010, 10, 77-84.	9.1	180
42	(Gold core)/(titania shell) nanostructures for plasmon-enhanced photon harvesting and generation of reactive oxygen species. Energy and Environmental Science, 2014, 7, 3431-3438.	30.8	180
43	Coupling between Molecular and Plasmonic Resonances in Freestanding Dyeâ~Gold Nanorod Hybrid Nanostructures. Journal of the American Chemical Society, 2008, 130, 6692-6693.	13.7	179
44	Glutathione- and Cysteine-Induced Transverse Overgrowth on Gold Nanorods. Journal of the American Chemical Society, 2007, 129, 6402-6404.	13.7	178
45	Advanced Plasmonic Materials for Dynamic Color Display. Advanced Materials, 2018, 30, e1704338.	21.0	176
46	Time–Temperature Indicator for Perishable Products Based on Kinetically Programmable Ag Overgrowth on Au Nanorods. ACS Nano, 2013, 7, 4561-4568.	14.6	173
47	Angle- and Energy-Resolved Plasmon Coupling in Gold Nanorod Dimers. ACS Nano, 2010, 4, 3053-3062.	14.6	158
48	Growth of Monodisperse Gold Nanospheres with Diameters from 20 nm to 220 nm and Their Core/Satellite Nanostructures. Advanced Optical Materials, 2014, 2, 65-73.	7.3	158
49	Emerging Applications of Plasmons in Driving CO ₂ Reduction and N ₂ Fixation. Advanced Materials, 2018, 30, e1802227.	21.0	155
50	A General Route to Diverse Mesoporous Metal Oxide Submicrospheres with Highly Crystalline Frameworks. Angewandte Chemie - International Edition, 2008, 47, 8682-8686.	13.8	149
51	Nanonecklaces assembled from gold rods, spheres, and bipyramids. Chemical Communications, 2007, , 1816.	4.1	146
52	Dielectric nanoresonators for light manipulation. Physics Reports, 2017, 701, 1-50.	25.6	145
53	Anisotropic Overgrowth of Metal Heterostructures Induced by a Site elective Silica Coating. Angewandte Chemie - International Edition, 2013, 52, 10344-10348.	13.8	139
54	Nanoscale surface chemistry directs the tunable assembly of silver octahedra into three two-dimensional plasmonic superlattices. Nature Communications, 2015, 6, 6990.	12.8	137

#	Article	IF	CITATIONS
55	Experimental Evidence of Plasmophores: Plasmon-Directed Polarized Emission from Gold Nanorod–Fluorophore Hybrid Nanostructures. Nano Letters, 2011, 11, 2296-2303.	9.1	135
56	Gold Nanobipyramid-Directed Growth of Length-Variable Silver Nanorods with Multipolar Plasmon Resonances. ACS Nano, 2015, 9, 7523-7535.	14.6	135
57	Gold Nanobipyramids: An Emerging and Versatile Type of Plasmonic Nanoparticles. Accounts of Chemical Research, 2019, 52, 2136-2146.	15.6	133
58	Shape-Dependent Refractive Index Sensitivities of Gold Nanocrystals with the Same Plasmon Resonance Wavelength. Journal of Physical Chemistry C, 2009, 113, 17691-17697.	3.1	130
59	(Gold Nanorod Core)/(Polyaniline Shell) Plasmonic Switches with Large Plasmon Shifts and Modulation Depths. Advanced Materials, 2014, 26, 3282-3289.	21.0	129
60	Growth of Gold Nanorods and Bipyramids Using CTEAB Surfactant. Journal of Physical Chemistry B, 2006, 110, 16377-16383.	2.6	127
61	Au/Ag core–shell nanocuboids for high-efficiency organic solar cells with broadband plasmonic enhancement. Energy and Environmental Science, 2016, 9, 898-905.	30.8	127
62	Observation of the Fano Resonance in Gold Nanorods Supported on High-Dielectric-Constant Substrates. ACS Nano, 2011, 5, 6754-6763.	14.6	124
63	Plasmon Coupling in Clusters Composed of Twoâ€Dimensionally Ordered Gold Nanocubes. Small, 2009, 5, 2111-2119.	10.0	119
64	Universal Scaling and Fano Resonance in the Plasmon Coupling between Gold Nanorods. ACS Nano, 2011, 5, 5976-5986.	14.6	119
65	Gold Nanobipyramidâ€Supported Silver Nanostructures with Narrow Plasmon Linewidths and Improved Chemical Stability. Advanced Functional Materials, 2016, 26, 341-352.	14.9	119
66	Photocurrent Enhancement of HgTe Quantum Dot Photodiodes by Plasmonic Gold Nanorod Structures. ACS Nano, 2014, 8, 8208-8216.	14.6	116
67	Pure Protein Scaffolds from Pickering High Internal Phase Emulsion Template. Macromolecular Rapid Communications, 2013, 34, 169-174.	3.9	114
68	Refractive Index Sensitivities of Noble Metal Nanocrystals: The Effects of Multipolar Plasmon Resonances and the Metal Type. Journal of Physical Chemistry C, 2011, 115, 7997-8004.	3.1	113
69	Metal Nanocrystalâ€Embedded Hollow Mesoporous TiO ₂ and ZrO ₂ Microspheres Prepared with Polystyrene Nanospheres as Carriers and Templates. Advanced Functional Materials, 2013, 23, 2137-2144.	14.9	112
70	Photon energy upconversion through thermal radiation with the power efficiency reaching 16%. Nature Communications, 2014, 5, 5669.	12.8	111
71	Nanoplasmonics. Chemical Society Reviews, 2014, 43, 3820.	38.1	107
72	Distinct Plasmonic Manifestation on Gold Nanorods Induced by the Spatial Perturbation of Small Gold Nanospheres. Nano Letters, 2012, 12, 1424-1430.	9.1	106

#	Article	IF	CITATIONS
73	Structure-Selective Synthesis of Mesostructured/Mesoporous Silica Nanofibers. Journal of the American Chemical Society, 2003, 125, 13966-13967.	13.7	105
74	Load-Independent Friction:Â MoO3Nanocrystal Lubricants. Journal of Physical Chemistry B, 1999, 103, 8405-8409.	2.6	102
75	Colloidal Moderateâ€Refractiveâ€Index Cu ₂ O Nanospheres as Visibleâ€Region Nanoantennas with Electromagnetic Resonance and Directional Lightâ€Scattering Properties. Advanced Materials, 2015, 27, 7432-7439.	21.0	102
76	Homogeneous Immunosorbent Assay Based on Single-Particle Enumeration Using Upconversion Nanoparticles for the Sensitive Detection of Cancer Biomarkers. Analytical Chemistry, 2018, 90, 4807-4814.	6.5	101
77	Active Electrochemical Plasmonic Switching on Polyaniline oated Gold Nanocrystals. Advanced Materials, 2017, 29, 1604862.	21.0	99
78	Effects of Dyes, Gold Nanocrystals, pH, and Metal Ions on Plasmonic and Molecular Resonance Coupling. Journal of the American Chemical Society, 2010, 132, 4806-4814.	13.7	97
79	Mass-Based Photothermal Comparison Among Gold Nanocrystals, PbS Nanocrystals, Organic Dyes, and Carbon Black. Journal of Physical Chemistry C, 2013, 117, 8909-8915.	3.1	97
80	Multiple Magnetic Mode-Based Fano Resonance in Split-Ring Resonator/Disk Nanocavities. ACS Nano, 2013, 7, 11071-11078.	14.6	97
81	Plasmon-Controlled Förster Resonance Energy Transfer. Journal of Physical Chemistry C, 2012, 116, 8287-8296.	3.1	96
82	Realization of Red Plasmon Shifts up to â^1⁄4900 nm by AgPd-Tipping Elongated Au Nanocrystals. Journal of the American Chemical Society, 2017, 139, 13837-13846.	13.7	96
83	One-Step Synthesis of Large-Aspect-Ratio Single-Crystalline Gold Nanorods by Using CTPAB and CTBAB Surfactants. Chemistry - A European Journal, 2007, 13, 2929-2936.	3.3	94
84	Heteroepitaxial Growth of Core–Shell and Core–Multishell Nanocrystals Composed of Palladium and Gold. Small, 2010, 6, 2566-2575.	10.0	94
85	Selective Pd Deposition on Au Nanobipyramids and Pd Siteâ€Dependent Plasmonic Photocatalytic Activity. Advanced Functional Materials, 2017, 27, 1700016.	14.9	94
86	Plasmon-induced modulation of the emission spectra of the fluorescent molecules near gold nanorods. Nanoscale, 2011, 3, 3849.	5.6	93
87	Cellular uptake behaviour, photothermal therapy performance, and cytotoxicity of gold nanorods with various coatings. Nanoscale, 2014, 6, 11462-11472.	5.6	92
88	Thickness Control Produces Gold Nanoplates with Their Plasmon in the Visible and Nearâ€Infrared Regions. Advanced Optical Materials, 2016, 4, 76-85.	7.3	91
89	The morphology and surface charge-dependent cellular uptake efficiency of upconversion nanostructures revealed by single-particle optical microscopy. Chemical Science, 2018, 9, 5260-5269.	7.4	91
90	Plasmonic Percolation: Plasmon-Manifested Dielectric-to-Metal Transition. ACS Nano, 2012, 6, 7162-7171.	14.6	89

#	Article	IF	CITATIONS
91	A Gold Nanocrystal/Poly(dimethylsiloxane) Composite for Plasmonic Heating on Microfluidic Chips. Advanced Materials, 2012, 24, 94-98.	21.0	88
92	Effect of the Dielectric Properties of Substrates on the Scattering Patterns of Gold Nanorods. ACS Nano, 2011, 5, 4865-4877.	14.6	87
93	Plasmonic–Molecular Resonance Coupling: Plasmonic Splitting versus Energy Transfer. Journal of Physical Chemistry C, 2012, 116, 14088-14095.	3.1	85
94	Bifunctional Au@Pt core–shell nanostructures for in situ monitoring of catalytic reactions by surface-enhanced Raman scattering spectroscopy. Nanoscale, 2014, 6, 9063-9070.	5.6	81
95	Curvature-Directed Assembly of Gold Nanocubes, Nanobranches, and Nanospheres. Langmuir, 2009, 25, 1692-1698.	3.5	80
96	Plasmonic Properties of Single Multispiked Gold Nanostars: Correlating Modeling with Experiments. Langmuir, 2012, 28, 8979-8984.	3.5	80
97	Single-Crystalline Gold Nanodisks on WS ₂ Mono- and Multilayers for Strong Coupling at Room Temperature. ACS Photonics, 2019, 6, 994-1001.	6.6	80
98	"Shipâ€inâ€aâ€Bottle―Growth of Noble Metal Nanostructures. Advanced Functional Materials, 2012, 22, 4526-4532.	14.9	77
99	Synthesis of Absorption-Dominant Small Gold Nanorods and Their Plasmonic Properties. Langmuir, 2015, 31, 7418-7426.	3.5	76
100	AgInS2/In2S3 heterostructure sensitization of Escherichia coli for sustainable hydrogen production. Nano Energy, 2018, 46, 234-240.	16.0	76
101	Colloidal Gold Nanocups with Orientationâ€Dependent Plasmonic Properties. Advanced Materials, 2016, 28, 6322-6331.	21.0	74
102	Au nanoparticle-embedded, nitrogen-deficient hollow mesoporous carbon nitride spheres for nitrogen photofixation. Journal of Materials Chemistry A, 2020, 8, 16218-16231.	10.3	74
103	Localized and Continuous Tuning of Monolayer MoS ₂ Photoluminescence Using a Single Shapeâ€Controlled Ag Nanoantenna. Advanced Materials, 2016, 28, 701-706.	21.0	73
104	Porous Pt Nanoparticles with High Nearâ€Infrared Photothermal Conversion Efficiencies for Photothermal Therapy. Advanced Healthcare Materials, 2016, 5, 3165-3172.	7.6	71
105	Enhanced CO ₂ reduction and valuable C ₂₊ chemical production by a CdS-photosynthetic hybrid system. Nanoscale, 2019, 11, 9296-9301.	5.6	71
106	Synthesis of Mesoporous Silica Nanofibers with Controlled Pore Architectures. Chemistry of Materials, 2004, 16, 5169-5181.	6.7	70
107	Coating fabrics with gold nanorods for colouring, UV-protection, and antibacterial functions. Nanoscale, 2013, 5, 788-795.	5.6	69
108	Nanoquartz in Late Permian C1 coal and the high incidence of female lung cancer in the Pearl River Origin area: a retrospective cohort study. BMC Public Health, 2008, 8, 398.	2.9	66

#	Article	IF	CITATIONS
109	Aerosol-Sprayed Gold/Ceria Photocatalyst with Superior Plasmonic Hot Electron-Enabled Visible-Light Activity. ACS Applied Materials & Interfaces, 2017, 9, 2560-2571.	8.0	65
110	Symmetryâ€Broken Au–Cu Heterostructures and their Tandem Catalysis Process in Electrochemical CO ₂ Reduction. Advanced Functional Materials, 2021, 31, 2101255.	14.9	64
111	Fano Resonance in (Gold Core)â^'(Dielectric Shell) Nanostructures without Symmetry Breaking. Small, 2012, 8, 1503-1509.	10.0	63
112	Emulsion-Templated Liquid Coreâ^'Polymer Shell Microcapsule Formation. Langmuir, 2009, 25, 2572-2574.	3.5	62
113	Resonanceâ€Couplingâ€Based Plasmonic Switches. Small, 2010, 6, 2514-2519.	10.0	62
114	Ultrasensitive Plasmonic Response of Bimetallic Au/Pd Nanostructures to Hydrogen. Advanced Functional Materials, 2014, 24, 7328-7337.	14.9	61
115	A Chemical Approach To Break the Planar Configuration of Ag Nanocubes into Tunable Two-Dimensional Metasurfaces. Nano Letters, 2016, 16, 3872-3878.	9.1	61
116	Biohybrid photoheterotrophic metabolism for significant enhancement of biological nitrogen fixation in pure microbial cultures. Energy and Environmental Science, 2019, 12, 2185-2191.	30.8	61
117	Photodriven Disproportionation of Nitrogen and Its Change to Reductive Nitrogen Photofixation. Angewandte Chemie - International Edition, 2021, 60, 927-936.	13.8	61
118	Nanopore Extrusion-Induced Transition from Spherical to Cylindrical Block Copolymer Micelles. Journal of the American Chemical Society, 2009, 131, 16650-16651.	13.7	60
119	A Schottkyâ€Barrierâ€Free Plasmonic Semiconductor Photocatalyst for Nitrogen Fixation in a "Oneâ€Stoneâ€Twoâ€Birds―Manner. Advanced Materials, 2022, 34, e2104226.	21.0	60
120	Macroscale Colloidal Noble Metal Nanocrystal Arrays and Their Refractive Indexâ€Based Sensing Characteristics. Small, 2014, 10, 802-811.	10.0	59
121	Unusual and Tunable One-Photon Nonlinearity in Gold-Dye Plexcitonic Fano Systems. Nano Letters, 2015, 15, 2705-2710.	9.1	59
122	Direct Monitoring of Cell Membrane Vesiculation with 2D AuNP@MnO ₂ Nanosheet Supraparticles at the Singleâ€Particle Level. Angewandte Chemie - International Edition, 2019, 58, 10542-10546.	13.8	58
123	Correlating the Plasmonic and Structural Evolutions during the Sulfidation of Silver Nanocubes. ACS Nano, 2013, 7, 9354-9365.	14.6	57
124	Understanding the roles of plasmonic Au nanocrystal size, shape, aspect ratio and loading amount in Au/g-C ₃ N ₄ hybrid nanostructures for photocatalytic hydrogen generation. Physical Chemistry Chemical Physics, 2018, 20, 22296-22307.	2.8	57
125	Dopamine-Mediated Assembly of Citrate-Capped Plasmonic Nanoparticles into Stable Core–Shell Nanoworms for Intracellular Applications. ACS Nano, 2019, 13, 5864-5884.	14.6	57
126	Crystalline structure-dependent growth of bimetallic nanostructures. Nanoscale, 2012, 4, 7070.	5.6	56

#	Article	IF	CITATIONS
127	Porous Carbon and Carbon/Metal Oxide Microfibers with Well-Controlled Pore Structure and Interface. Journal of the American Chemical Society, 2008, 130, 5034-5035.	13.7	55
128	Multifunctional Mesostructured Silica Microspheres from an Ultrasonic Aerosol Spray. Advanced Functional Materials, 2008, 18, 2956-2962.	14.9	53
129	Ultrasmall Mode Volumes in Plasmonic Cavities of Nanoparticleâ€Onâ€Mirror Structures. Small, 2016, 12, 5190-5199.	10.0	53
130	Aerosol-spray metal phosphide microspheres with bifunctional electrocatalytic properties for water splitting. Journal of Materials Chemistry A, 2018, 6, 4783-4792.	10.3	53
131	Synergistic Nanozymetic Activity of Hybrid Gold Bipyramid–Molybdenum Disulfide Core@Shell Nanostructures for Two-Photon Imaging and Anticancer Therapy. ACS Applied Materials & Interfaces, 2018, 10, 42068-42076.	8.0	53
132	Incorporation of Gold Nanorods and Their Enhancement of Fluorescence in Mesostructured Silica Thin Films. Journal of Physical Chemistry C, 2008, 112, 18895-18903.	3.1	52
133	Single-Crystal Mesoporous Silica Ribbons. Angewandte Chemie - International Edition, 2005, 44, 332-336.	13.8	50
134	Titania oated Gold Nanoâ€Bipyramids for Blocking Autophagy Flux and Sensitizing Cancer Cells to Proteasome Inhibitorâ€Induced Death. Advanced Science, 2018, 5, 1700585.	11.2	50
135	Electrochemically controlled metasurfaces with high-contrast switching at visible frequencies. Science Advances, 2021, 7, .	10.3	49
136	Metallic-Phase MoS ₂ Nanopetals with Enhanced Electrocatalytic Activity for Hydrogen Evolution. ACS Sustainable Chemistry and Engineering, 2018, 6, 13435-13442.	6.7	48
137	Circular Gold Nanodisks with Synthetically Tunable Diameters and Thicknesses. Advanced Functional Materials, 2018, 28, 1705516.	14.9	47
138	Comparison of the plasmonic performances between lithographically fabricated and chemically grown gold nanorods. Physical Chemistry Chemical Physics, 2015, 17, 10861-10870.	2.8	46
139	Pd films on soft substrates: a visual, high-contrast and low-cost optical hydrogen sensor. Light: Science and Applications, 2019, 8, 4.	16.6	46
140	Site-Selective Deposition of Metal–Organic Frameworks on Gold Nanobipyramids for Surface-Enhanced Raman Scattering. Nano Letters, 2021, 21, 8205-8212.	9.1	46
141	Role of shape in substrate-induced plasmonic shift and mode uncovering on gold nanocrystals. Nanoscale, 2016, 8, 17645-17657.	5.6	45
142	Self-assembly of Au@Ag core–shell nanocuboids into staircase superstructures by droplet evaporation. Nanoscale, 2018, 10, 142-149.	5.6	44
143	Magnetic Plasmon-Enhanced Second-Harmonic Generation on Colloidal Gold Nanocups. Nano Letters, 2019, 19, 2005-2011.	9.1	44
144	Directional Control of Light with Nanoantennas. Advanced Optical Materials, 2021, 9, .	7.3	44

#	Article	IF	CITATIONS
145	Ultrasonic aerosol spray-assisted preparation of TiO2/In2O3 composite for visible-light-driven photocatalysis. Journal of Catalysis, 2014, 310, 84-90.	6.2	43
146	Room temperature synthesis of a highly active Cu/Cu ₂ O photocathode for photoelectrochemical water splitting. Journal of Materials Chemistry A, 2016, 4, 13736-13741.	10.3	43
147	Aerosol-spray diverse mesoporous metal oxides from metal nitrates. Scientific Reports, 2015, 5, 9923.	3.3	42
148	Nanoantennaâ€Sandwiched Graphene with Giant Spectral Tuning in the Visibleâ€ŧoâ€Nearâ€Infrared Region. Advanced Optical Materials, 2014, 2, 162-170.	7.3	39
149	Polydopamine-based concentric nanoshells with programmable architectures and plasmonic properties. Nanoscale, 2017, 9, 16968-16980.	5.6	39
150	Colloidal Gold Nanorings and Their Plasmon Coupling with Gold Nanospheres. Small, 2019, 15, e1902608.	10.0	39
151	Single-Particle Emission Spectroscopy Resolves d-Hole Relaxation in Copper Nanocubes. ACS Energy Letters, 2019, 4, 2458-2465.	17.4	39
152	Gold nanobipyramid-loaded black phosphorus nanosheets for plasmon-enhanced photodynamic and photothermal therapy of deep-seated orthotopic lung tumors. Acta Biomaterialia, 2020, 107, 260-271.	8.3	39
153	How to Utilize Excited Plasmon Energy Efficiently. ACS Nano, 2021, 15, 10759-10768.	14.6	39
154	Plasmonic Goldâ^'Superparamagnetic Hematite Heterostructures. Langmuir, 2011, 27, 5071-5075.	3.5	38
155	Plasmonically enabled two-dimensional material-based optoelectronic devices. Nanoscale, 2020, 12, 8095-8108.	5.6	38
156	Gold nanobipyramid-embedded ultrathin metal nanoframes for <i>in situ</i> monitoring catalytic reactions. Chemical Science, 2020, 11, 3198-3207.	7.4	35
157	Extraordinary Surface Plasmon Coupled Emission Using Core/Shell Gold Nanorods. Journal of Physical Chemistry C, 2012, 116, 9259-9264.	3.1	34
158	Gold Nanobipyramidâ€Enhanced Hydrogen Sensing with Plasmon Red Shifts Reaching â‰^140 nm at 2 vol% Hydrogen Concentration. Advanced Optical Materials, 2017, 5, 1700740.	7.3	34
159	Colour routing with single silver nanorods. Light: Science and Applications, 2019, 8, 39.	16.6	34
160	Optical Fiber-Excited Surface Plasmon Resonance Spectroscopy of Single and Ensemble Gold Nanorods. Journal of Physical Chemistry C, 2008, 112, 8105-8109.	3.1	33
161	Tetrakis(4â€sulfonatophenyl)porphyrinâ€Directed Assembly of Gold Nanocrystals: Tailoring the Plasmon Coupling Through Controllable Gap Distances. Small, 2010, 6, 2001-2009.	10.0	33
162	Plasmon-Modulated Light Scattering from Gold Nanocrystal-Decorated Hollow Mesoporous Silica Microspheres. ACS Nano, 2010, 4, 6565-6572.	14.6	33

#	Article	IF	CITATIONS
163	Asymmetric growth of Au-core/Ag-shell nanorods with a strong octupolar plasmon resonance and an efficient second-harmonic generation. Nano Research, 2018, 11, 686-695.	10.4	33
164	Coupling between the Mie Resonances of Cu ₂ O Nanospheres and the Excitons of Dye Aggregates. ACS Photonics, 2018, 5, 3838-3848.	6.6	33
165	Switching plasmon coupling through the formation of dimers from polyaniline-coated gold nanospheres. Nanoscale, 2015, 7, 12516-12526.	5.6	32
166	Concave gold bipyramids bound with multiple high-index facets: improved Raman and catalytic activities. Nanoscale, 2017, 9, 5879-5886.	5.6	32
167	Infraredâ€Responsive Colloidal Silver Nanorods for Surfaceâ€Enhanced Infrared Absorption. Advanced Optical Materials, 2018, 6, 1800436.	7.3	32
168	Fabrication of Au nanotube arrays and their plasmonic properties. Nanoscale, 2013, 5, 3742.	5.6	31
169	Colloidal porous gold nanoparticles. Nanoscale, 2018, 10, 18473-18481.	5.6	31
170	Dual templating synthesis of hierarchical porous silica materials with three orders of length scale. Chemical Communications, 2010, 46, 8767.	4.1	30
171	Highly sensitive and uniform surface-enhanced Raman spectroscopy from grating-integrated plasmonic nanograss. Nanoscale Horizons, 2016, 1, 290-297.	8.0	30
172	Loading Metal Nanostructures on Cotton Fabrics as Recyclable Catalysts. Small, 2013, 9, 1003-1007.	10.0	29
173	Largeâ€Area Patterning of Metal Nanostructures by Dipâ€Pen Nanodisplacement Lithography for Optical Applications. Small, 2017, 13, 1702003.	10.0	29
174	Ultraviolet–Visible Chiroptical Activity of Aluminum Nanostructures. Small, 2017, 13, 1701112.	10.0	29
175	Selective Heteroepitaxial Nanocrystal Growth of Rare Earth Fluorides on Sodium Chloride: Synthesis and Density Functional Calculations. Angewandte Chemie - International Edition, 2012, 51, 8796-8799.	13.8	28
176	Plasmon Modes Induced by Anisotropic Gap Opening in Au@Cu ₂ O Nanorods. Small, 2016, 12, 4264-4276.	10.0	28
177	Electrochemical Switching of Plasmonic Colors Based on Polyaniline-Coated Plasmonic Nanocrystals. ACS Applied Materials & Interfaces, 2020, 12, 17733-17744.	8.0	28
178	A wide-spectrum-responsive TiO 2 photoanode for photoelectrochemical cells. Applied Catalysis B: Environmental, 2015, 168-169, 483-489.	20.2	27
179	Plasmonic Color Laser Printing inside Transparent Gold Nanodiskâ€Embedded Poly(dimethylsiloxane) Matrices. Advanced Optical Materials, 2020, 8, 1901605.	7.3	27
180	Anapole States and Toroidal Resonances Realized in Simple Gold Nanoplateâ€onâ€Mirror Structures. Advanced Optical Materials, 2020, 8, 2001173.	7.3	27

#	Article	IF	CITATIONS
181	Plasmon-enabled N ₂ photofixation on partially reduced Ti ₃ C ₂ MXene. Chemical Science, 2021, 12, 11213-11224.	7.4	27
182	Transverse oxidation of gold nanorods assisted by selective end capping of silver oxide. Journal of Materials Chemistry, 2011, 21, 11537.	6.7	26
183	Mechanically tunable sub-10 nm metal gap by stretching PDMS substrate. Nanotechnology, 2017, 28, 075301.	2.6	26
184	Fluorescent Mesostructured Polythiophene–Silica Composite Particles Synthesized by in Situ Polymerization of Structure-Directing Monomers. Chemistry of Materials, 2007, 19, 6222-6229.	6.7	25
185	The use of femto-second lasers to trigger powerful explosions of gold nanorods to destroy cancer cells. Biomaterials, 2013, 34, 6157-6162.	11.4	25
186	Highly enhanced transverse plasmon resonance and tunable double Fano resonances in gold@titania nanorods. Nanoscale, 2016, 8, 6514-6526.	5.6	25
187	Laser illumination-induced dramatic catalytic activity change on Au nanospheres. Chemical Science, 2019, 10, 5793-5800.	7.4	25
188	Hydrothermal transformation from Au core–sulfide shell to Au nanoparticle-decorated sulfide hybrid nanostructures. Nanoscale, 2010, 2, 1650.	5.6	24
189	Broadside Nanoantennas Made of Single Silver Nanorods. ACS Nano, 2018, 12, 1720-1731.	14.6	24
190	Molecular Tunnel Junction-Controlled High-Order Charge Transfer Plasmon and Fano Resonances. ACS Nano, 2018, 12, 12541-12550.	14.6	24
191	Gold nanonails for surface-enhanced infrared absorption. Nanoscale Horizons, 2020, 5, 1200-1212.	8.0	24
192	CTAB-coated gold nanorods elicit allergic response through degranulation and cell death in human basophils. Nanoscale, 2012, 4, 4447.	5.6	22
193	Insight into factors affecting the presence, degree, and temporal stability of fluorescence intensification on ZnO nanorod ends. Nanoscale, 2015, 7, 1424-1436.	5.6	22
194	Antiangiogenesis-Combined Photothermal Therapy in the Second Near-Infrared Window at Laser Powers Below the Skin Tolerance Threshold. Nano-Micro Letters, 2019, 11, 93.	27.0	22
195	Crown monitoring: Trace the dynamic changes of caspase-3 and H2O2 in real-time imaging based on FRET/SERS. Biosensors and Bioelectronics, 2021, 192, 113539.	10.1	22
196	What Morphologies Do We Want? – TEM Images from Dilute Diblock Copolymer Solutions. Macromolecular Chemistry and Physics, 2011, 212, 663-672.	2.2	21
197	Anisotropic Overgrowth of Metal Heterostructures Induced by a Siteâ€Selective Silica Coating. Angewandte Chemie, 2013, 125, 10534-10538.	2.0	21
198	Chirality-selective transparency induced by lattice resonance in bilayer metasurfaces. Photonics Research, 2021, 9, 484.	7.0	21

#	Article	IF	CITATIONS
199	Heterostructures Built through Siteâ€&elective Deposition on Anisotropic Plasmonic Metal Nanocrystals and Their Applications. Small Structures, 2021, 2, .	12.0	21
200	Direct encoding of silica submicrospheres with cadmium telluride nanocrystals. Journal of Materials Chemistry, 2009, 19, 7002.	6.7	20
201	AlPcS-loaded gold nanobipyramids with high two-photon efficiency for photodynamic therapy <i>in vivo</i> . Nanoscale, 2019, 11, 3386-3395.	5.6	20
202	Au Nanobottles with Synthetically Tunable Overall and Opening Sizes for Chemo-Photothermal Combined Therapy. ACS Applied Materials & Interfaces, 2019, 11, 5353-5363.	8.0	19
203	Switching plasmonic Fano resonance in gold nanosphere–nanoplate heterodimers. Nanoscale, 2019, 11, 9641-9653.	5.6	19
204	Plasmonic and sensing properties of vertically oriented hexagonal gold nanoplates. Nanoscale, 2018, 10, 15058-15070.	5.6	18
205	Strengthening Fano resonance on gold nanoplates with gold nanospheres. Nanoscale, 2020, 12, 1975-1984.	5.6	18
206	All-State Switching of the Mie Resonance of Conductive Polyaniline Nanospheres. Nano Letters, 2022, 22, 1406-1414.	9.1	18
207	Deep Fano resonance with strong polarization dependence in gold nanoplate–nanosphere heterodimers. Nanoscale, 2017, 9, 13222-13234.	5.6	17
208	Chemically functionalized graphene/polymer nanocomposites as light heating platform. Polymer Composites, 2016, 37, 1350-1358.	4.6	15
209	(Metal yolk)/(porous ceria shell) nanostructures for high-performance plasmonic photocatalysis under visible light. Nano Research, 2020, 13, 1354-1362.	10.4	15
210	Molecular Sensitivities of Substrate-Supported Gold Nanocrystals. Journal of Physical Chemistry C, 2019, 123, 7336-7346.	3.1	14
211	Generation and Detection of Strain-Localized Excitons in WS ₂ Monolayer by Plasmonic Metal Nanocrystals. ACS Nano, 2022, 16, 10647-10656.	14.6	14
212	Chemically Synthesized Electromagnetic Metal Oxide Nanoresonators. Advanced Optical Materials, 2019, 7, 1900396.	7.3	13
213	Electrochemical coating of different conductive polymers on diverse plasmonic metal nanocrystals. Nanoscale, 2020, 12, 21617-21623.	5.6	13
214	Metal-free g-C ₃ N ₄ nanosheets as a highly visible-light-active photocatalyst for thiol–ene reactions. Nanoscale, 2021, 13, 3493-3499.	5.6	13
215	Vesicle Array-Templated Large-Area Silica Surface Patterns. Journal of the American Chemical Society, 2005, 127, 10154-10155.	13.7	12
216	Formation of Different Gold Nanocrystal Core–Resin Shell Structures through the Control of the Core Assembly and Shell Polymerization. Langmuir, 2012, 28, 9082-9092.	3.5	12

#	Article	IF	CITATIONS
217	Dislocated Double-Layered Metal Gratings: Refractive Index Sensors with High Figure of Merit. Plasmonics, 2015, 10, 1489-1497.	3.4	12
218	Growth of Au Hollow Stars and Harmonic Excitation Energy Transfer. ACS Nano, 2020, 14, 736-745.	14.6	12
219	Photodriven Disproportionation of Nitrogen and Its Change to Reductive Nitrogen Photofixation. Angewandte Chemie, 2021, 133, 940-949.	2.0	12
220	A novel deposition mechanism of Au on Ag nanostructures involving galvanic replacement and reduction reactions. Chemical Communications, 2021, 57, 8332-8335.	4.1	12
221	Selective Deposition of Catalytic Metals on Plasmonic Au Nanocups for Room-Light-Active Photooxidation of <i>o</i> -Phenylenediamine. ACS Applied Materials & Interfaces, 2021, 13, 51855-51866.	8.0	12
222	Driving Click Reactions with Plasmonic Hot Holes on (Au Core)@(Cu ₂ O Shell) Nanostructures for Regioselective Production of 1,2,3-Triazoles. ACS Applied Nano Materials, 2021, 4, 4623-4631.	5.0	12
223	Room-temperature metal-activator-free phosphorescence from mesoporous silica. Physical Chemistry Chemical Physics, 2011, 13, 2387-2393.	2.8	11
224	Strong magnetic resonances and largely enhanced second-harmonic generation of colloidal MoS2 and ReS2@Au nanoantennas with assembled 2D nanosheets. Nanoscale, 2018, 10, 124-131.	5.6	11
225	Substrate-Enabled Plasmonic Color Switching with Colloidal Gold Nanorings. , 2020, 2, 744-753.		11
226	Electromagnetic Resonanceâ€Modulated Magnetic Emission in Europiumâ€Doped Subâ€Micrometer Zirconia Spheres. Advanced Optical Materials, 2021, 9, 2002212.	7.3	11
227	Effects of shape and solute-solvent compatibility on the efficacy of chirality transfer: Nanoshapes in nematics. Science Advances, 2022, 8, eabl4385.	10.3	11
228	General Method for Determining Light Scattering and Absorption of Nanoparticle Composites. Advanced Optical Materials, 2019, 7, 1801315.	7.3	10
229	Detection of cell-surface sialic acids and photodynamic eradication of cancer cells using dye-modified polydopamine-coated gold nanobipyramids. Journal of Materials Chemistry B, 2021, 9, 5780-5784.	5.8	10
230	Facet- and Gas-Dependent Reshaping of Au Nanoplates by Plasma Treatment. ACS Nano, 2021, 15, 9860-9870.	14.6	9
231	Titanium Oxynitride Spheres with Broad Plasmon Resonance for Solar Seawater Desalination. ACS Applied Materials & Interfaces, 2022, 14, 28769-28780.	8.0	9
232	Porous upconversion materials-assisted near infrared energy harvesting by chlorophylls. Chemical Communications, 2011, 47, 3511.	4.1	8
233	Efficiency enhancement of organic photovoltaics by introducing high-mobility curved small-molecule semiconductors as additives. Journal of Materials Chemistry A, 2019, 7, 12740-12750.	10.3	8
234	(Gold nanorod core)/(poly(3,4-ethylene-dioxythiophene) shell) nanostructures and their monolayer arrays for plasmonic switching. Nanoscale, 2020, 12, 20684-20692.	5.6	8

#	Article	IF	CITATIONS
235	Asymmetric Light Scattering on Heterodimers Made of Au Nanorods Vertically Standing on Au Nanodisks. Advanced Optical Materials, 2021, 9, 2001595.	7.3	8
236	Multiphoton Photoluminescence in Hybrid Plasmon–Fiber Cavities with Au and Au@Pd Nanobipyramids: Two-Photon versus Four-Photon Processes and Rapid Quenching. ACS Photonics, 2021, 8, 2088-2094.	6.6	8
237	Sophisticated plasmon-enhanced photo-nanozyme for anti-angiogenic and tumor-microenvironment-responsive combinatorial photodynamic and photothermal cancer therapy. Journal of Industrial and Engineering Chemistry, 2021, 104, 106-106.	5.8	8
238	Importance of substrates for the visibility of "dark" plasmonic modes. Optics Express, 2020, 28, 13938.	3.4	8
239	Giant Second Harmonic Generation Enhancement in a High- <i>Q</i> Doubly Resonant Hybrid Plasmon–Fiber Cavity System. ACS Nano, 2021, 15, 19409-19417.	14.6	8
240	Effects of crystallographic facet-specific peptide adsorption along single ZnO nanorods on the characteristic fluorescence intensification on nanorod ends (FINE) phenomenon. Nanoscale, 2015, 7, 18813-18826.	5.6	7
241	Slow Charge Carrier Relaxation in Gold Nanoparticles. Journal of Physical Chemistry C, 2020, 124, 24322-24330.	3.1	7
242	Plasmonâ€Enhanced, Selfâ€Traced Nanomotors on the Surface of Silicon. Angewandte Chemie - International Edition, 2021, 60, 24958-24967.	13.8	7
243	Monosteps on the Surfaces of Mesostructured Silica and Titania Thin Films. Small, 2010, 6, 1880-1885.	10.0	6
244	Disentangling Light- and Temperature-Induced Thermal Effects in Colloidal Au Nanoparticles. Journal of Physical Chemistry C, 2022, 126, 3591-3599.	3.1	6
245	Alignment Control of Polythiophene Chains with Mesostructured Silica Nanofibers Having Different Pore Orientations. Small, 2012, 8, 2021-2026.	10.0	5
246	Electrocatalytic glycerol oxidation enabled by surface plasmon polariton-induced hot carriers in Kretschmann configuration. Nanoscale, 2019, 11, 23234-23240.	5.6	5
247	Substrateâ€Modulated Electromagnetic Resonances in Colloidal Cu 2 O Nanospheres. Particle and Particle Systems Characterization, 2020, 37, 2000106.	2.3	5
248	Electrophoretic Plasmonic Ink for Dynamic Color Display. Advanced Optical Materials, 2021, 9, 2100091.	7.3	5
249	Gold Nanocups: Colloidal Gold Nanocups with Orientationâ€Đependent Plasmonic Properties (Adv.) Tj ETQq1 1 ().784314 21.0	rg&T /Overloc
250	Surface-enhanced infrared absorption. Scientia Sinica: Physica, Mechanica Et Astronomica, 2019, 49, 124204.	0.4	3
251	Direct deposition of anatase TiO2 on thermally unstable gold nanobipyramid: Morphology-conserved plasmonic nanohybrid for combinational photothermal and photocatalytic cancer therapy. Applied Materials Today, 2022, 27, 101472.	4.3	3
252	Mode-dependent energy exchange between near- and far-field through silicon-supported single silver nanorods. Nanoscale, 2022, 14, 8362-8373.	5.6	3

#	Article	IF	CITATIONS
253	Tetrakis(4-sulfonatophenyl)porphyrin-Directed Assembly of Gold Nanocrystals: Tailoring the Plasmon Coupling Through Controllable Gap Distances. Small, 2010, 6, n/a-n/a.	10.0	2
254	Optotransfection of mammalian cells based on a femtosecond laser and facilitated by gold nanorods. Nanotechnology, 2013, 24, 435102.	2.6	2
255	Plasmon-assisted Chemical Reactions. World Scientific Series in Nanoscience and Nanotechnology, 2016, , 155-193.	0.1	1
256	Nanostructures: Ultraviolet–Visible Chiroptical Activity of Aluminum Nanostructures (Small 39/2017). Small, 2017, 13, .	10.0	1
257	A new cobalt(<scp>ii</scp>) complex nanosheet as an electroactive medium for plasmonic switching on Au nanoparticles. Dalton Transactions, 2021, 50, 15900-15905.	3.3	1
258	Functional Metal Nanocrystals for Biomedical Applications. , 2017, , 809-840.		1
259	Electronic structures of [Ln(NO3)x(NCS)y]nâ^' (Ln â‰; La, Nd, Er). Journal of Alloys and Compounds, 1996, 233, 52-55.	5.5	0
260	Plasmonic switches: Resonance-Coupling-Based Plasmonic Switches (Small 22/2010). Small, 2010, 6, 2474-2474.	10.0	0
261	Plasmon Coupling between Colloidal Gold Nanorods. , 2013, , .		0
262	Hong Kong: An R&D Hub in Asia for Materials Science and Engineering. Advanced Materials, 2014, 26, 5235-5238.	21.0	0
263	Plasmon Switching: Active Electrochemical Plasmonic Switching on Polyanilineâ€Coated Gold Nanocrystals (Adv. Mater. 8/2017). Advanced Materials, 2017, 29, .	21.0	0
264	Plasmonâ€Enhanced, Selfâ€Traced Nanomotors on the Surface of Silicon. Angewandte Chemie, 0, , .	2.0	0
265	Directional Control of Light with Nanoantennas (Advanced Optical Materials 1/2021). Advanced Optical Materials, 2021, 9, 2170002.	7.3	0
266	Functional Metal Nanocrystals for Biomedical Applications. , 2015, , 1-32.		0
267	Gold/Ceria Nanostructures for Plasmon-Enhanced Catalytic Reactions Under Visible Light. ECS Meeting Abstracts, 2017, , .	0.0	0
268	(Invited) Plasmonic Driving of Chemical Reactions. ECS Meeting Abstracts, 2017, , .	0.0	0
269	Anisotropic Plasmonic Light Scattering. , 2018, , .		0
270	(Invited) Plasmon-Driven Chemical Reactions. ECS Meeting Abstracts, 2019, , .	0.0	0

#	Article	IF	CITATIONS
271	Synthesis and Functionalization of Anisotropic Silver Nanoparticles. , 2022, , 349-396.		0